

SCALING STRUCTURED MULTIGRID TO 500K+ CORES THROUGH COARSE-GRID REDISTRIBUTION*

ANDREW REISNER[†], LUKE N. OLSON^{*}, AND J. DAVID MOULTON[‡]

Abstract. The efficient solution of sparse, linear systems resulting from the discretization of partial differential equations is crucial to the performance of many physics-based simulations. The algorithmic optimality of multilevel approaches for common discretizations makes them a good candidate for an efficient parallel solver. Yet, modern architectures for high-performance computing systems continue to challenge the parallel scalability of multilevel solvers. While algebraic multigrid methods are robust for solving a variety of problems, the increasing importance of data locality and cost of data movement in modern architectures motivates the need to carefully exploit structure in the problem.

Robust logically structured variational multigrid methods, such as Black Box Multigrid (BoxMG), maintain structure throughout the multigrid hierarchy. This avoids indirection and increased coarse-grid communication costs typical in parallel algebraic multigrid. Nevertheless, the parallel scalability of structured multigrid is challenged by coarse-grid problems where the overhead in communication dominates computation. In this paper, an algorithm is introduced for redistributing coarse-grid problems through incremental agglomeration. Guided by a predictive performance model, this algorithm provides robust redistribution decisions for structured multilevel solvers.

A two-dimensional diffusion problem is used to demonstrate the significant gain in performance of this algorithm over the previous approach that used agglomeration to one processor. In addition, the parallel scalability of this approach is demonstrated on two large-scale computing systems, with solves on up to 500K+ cores.

Key words. multigrid, structure, parallel, scalability, stencil

AMS subject classifications. 65F50, 65Y05, 65N55

1. Introduction. The efficient solution of large, sparse linear systems resulting from the discretization of elliptic partial differential equations (PDEs) is crucial to the performance of many numerical simulations. Although there has been significant progress in developing general Algebraic Multigrid (AMG) solvers [27], modern high-performance computing (HPC) architectures continue to pose significant challenges to parallel scalability and performance (e.g., [3, 13, 5]). These challenges include reducing data movement, increasing arithmetic intensity, and identifying opportunities to improve resilience, and are more readily addressed in settings where problem structure can be identified and exploited. For example, robust structured variational multigrid methods, such as Black Box Multigrid (BoxMG) [10, 11], take advantage of direct memory addressing and fixed stencil patterns throughout the multigrid hierarchy to realize a $10\times$ speed-up over AMG for heterogeneous diffusion problems [20]. In addition, the communication patterns in a parallel BoxMG solve are fixed and predictable throughout the multigrid hierarchy. Here we explore using this information to improve the parallel scalability and performance of elliptic solves for problems with structure.

The meshing strategy used in the discretization of a PDE has a significant impact on the amount of structure that can be exploited by the solver. For example, single-block locally structured grids can be body fitted to capture smooth non-planar geometries [9], and can use embedded boundary discretization techniques to add additional flexibility to the representation of object boundaries. Robust structured vari-

*LOS ALAMOS REPORT LA-UR-17-22886

[†]Department of Computer Science, University of Illinois at Urbana-Champaign.

[‡]Applied Mathematics and Plasma Physics, Los Alamos National Laboratory.

ational methods, such as BoxMG, are directly applicable to these cases. In contrast, fully unstructured grids can capture very complex geometries, including non-smooth features over a range of scales, but demand general algebraic multilevel solvers, such as AMG or smoothed aggregation AMG. The needs of many applications lie between these extremes, and a variety of adaptive or multi-mesh strategies have been developed to preserve structure and enable its use in the discretization and solver. These approaches generally lead to specialized hybrid solvers, favoring structured techniques at higher levels of refinement and algebraic techniques below a suitably chosen coarse level [25]. While these hybrid solvers present a variety of challenges, a single-block logically structured solver is a critical component of their design and performance.

A common approach to parallel multigrid solvers for PDEs is to partition the spatial domain across available processor cores. However, on coarser levels, the local problem size decreases and the communication cost begins to impact parallel performance. A natural approach to alleviate this problem is to gather the coarsest problem to a single processor (or redundantly to all the processors), and to solve it with a serial multigrid cycle. This approach was first motivated by a performance model of early distributed memory clusters [14] where core counts were quite small, and it was used in the initial version of parallel BoxMG. Unfortunately, as the weak scaling study in Figure 1 shows, this approach scales linearly with the number of cores, and hence, is not practical for modern systems. A modification of this approach that gathers the coarse problem to a multi-core node [23], and then leverages OpenMP threading on that node, improves the performance but does not address the scaling. This challenge of reducing communication costs at coarser levels is even more acute in AMG methods, and this led to exploration of agglomeration to redundant coarse problems at higher levels [3], as well as redistribution of smaller portions of the coarse problem to enhance scalability [13], leading to approximately $2\times$ speedup in the solve phase.

An alternative to this two-level gather-to-one approach is a more conservative redistribution strategy that can be applied recursively as the problem is coarsened. In single-block structured solvers, the decision to redistribute data is driven by balancing communication costs in relaxation with diminishing local work. This approach was first considered in a structured setting [28], and used a heuristic to guide recursive application of nearest neighbor agglomeration. Later, in the Los Alamos AMG (LAMG) solver, a heuristic was developed to guide the reduction of the number of active cores at each level by a power of two [17]. In this paper, an optimized redistribution algorithm is proposed for robust structured multigrid methods that balances the computation and communication costs at each level. The structured setting enables the enumeration of possible coarse-grid configurations, and a performance model is developed to support optimization of the coarsening path that is selected through these configurations. The utility of this approach is demonstrated through scaling studies extending beyond 100K cores on two modern supercomputers.

The remainder of this paper is organized as follows. Section 2 highlights relevant features of robust variational multigrid methods, examines the domain decomposition implementation in BoxMG, and proposes a redistribution algorithm that can be applied recursively. The performance model for this parallel algorithm with redistribution is developed in Section 3, and the optimization algorithm is presented in Section 4. Scaling studies are presented in Section 5 demonstrating the efficacy of the proposed method, and Section 6 gives conclusions.

2. Robust Variational Multigrid on Structured Grids. In the case of a symmetric, positive definite matrix problem, a Galerkin (variational) coarse-grid op-

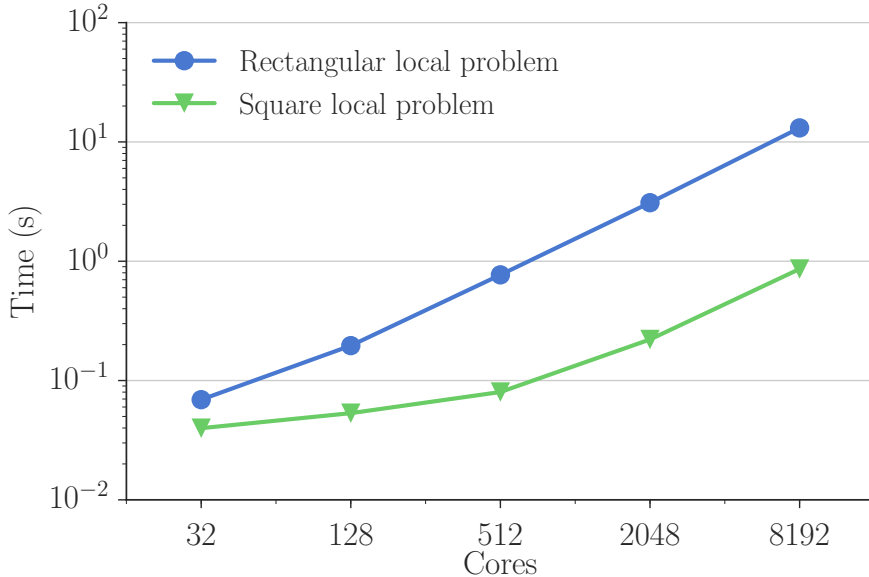


FIG. 1. Weak scaling on Blue Waters for a local problem size of 568×71 (rectangular) and 200×200 (square) using $V(2,1)$ -cycles with a gather-to-one serial BoxMG coarse-grid solver.

erator is effective in defining the coarse-level problems because it minimizes the error in the range of interpolation [7]. This variational operator is formed as the triple matrix product of the restriction (transpose of interpolation), the fine-grid operator, and the interpolation, making it well suited for black box and algebraic multilevel solver algorithms. In the case of structured grids, the complexity of the coarse-grid operators is bounded, and the stencil pattern can be fixed *a priori*.

However, in this approach, the interpolation must be sufficiently accurate to ensure the variational coarse-grid operator satisfies the approximation property [27]. For example, in two-dimensional diffusion problems with discontinuous coefficients, bilinear interpolation is not accurate across discontinuities because the gradient of the solution is not continuous. Thus, a key element in robust multigrid methods is *operator-induced* interpolation [8, 27], which uses the matrix problem to construct intergrid transfer operators. In the case of structured grid problems, operator-induced interpolation is naturally motivated by noting the normal component of the flux is continuous [10], and its impact on the properties of the variational coarse-grid operator is understood through its connection to homogenization [22, 19]. This approach has natural extensions to non-symmetric problems as well [11, 29].

Robust methods also require careful consideration of the smoothing operator. Although, Gauss-Seidel is effective for many problems, anisotropy often demands alternating line smoothing or plane smoothing [8, 27]. With coarse-grid operators and interpolation defined, a standard multigrid cycling is used, for example a V-cycle as in Algorithm 1.

In this paper, interpolation and coarse-grid operators are constructed using the implementation in BoxMG [1, 10, 22] with standard coarsening by a factor of 2, however the approach applies to any structured method. BoxMG is used because its operator-induced interpolation is designed to handle discontinuous coefficients, and additional heuristics ensure optimal performance for Dirichlet, Neumann and

Algorithm 1: Multilevel V-cycle

Input: x_{L-1} fine-grid initial guess
 b_{L-1} fine-grid right-hand side
 A_0, \dots, A_{L-1}
 P_1, \dots, P_{L-1}

Output: x_{L-1} fine-grid iterative solution

```

1 for  $l = L - 1, \dots, 1$  do
2    $\text{relax}(A_l, x_l, b_l, \nu_1)$  {relax  $\nu_1$  times}
3    $r_l = b_l - A_l x_l$  {compute residual}
4    $b_{l-1} = P_l^T r_l$  {restrict residual}
5  $x_0 = \text{solve}(A_0, b_0)$  {coarse-grid direct solve}
6 for  $l = 1, \dots, L - 1$  do
7    $x_l = x_l + P_l x_{l-1}$  {interpolate and correct}
8    $\text{relax}(A_l, x_l, b_l, \nu_2)$  {relax  $\nu_2$  times}

```

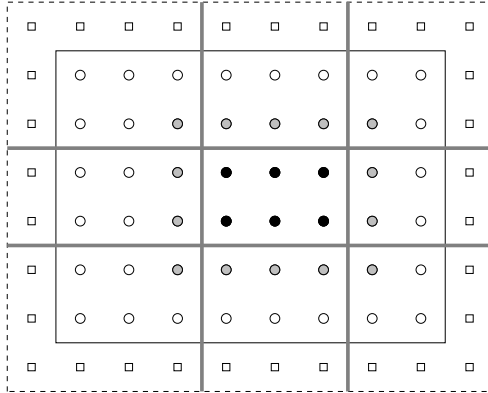


FIG. 2. Domain partition. Circles represent degrees of freedom, with \bullet denoting points on process k , \circ representing halo points needed for communication from other processors, and \circ points on other processors.

Robin boundary conditions on logically structured grids of any dimension (i.e., it is not restricted to grids $2^k + 1$). In addition, only the fine-grid problem is specified; coarse-grid operators are constructed through the variational (Galerkin) product. The package is also released as open source in the Cedar Project [21].

2.1. Domain Decomposition Parallel Implementation. The distributed memory parallel implementation of BoxMG divides the problem domain among available processors. The processors are arranged in a structured grid and points in the fine grid problem are divided among processors in each dimension — see Figure 2. Since the computation is structured, inter-process communication occurs through nearest neighbor halo updates with a halo width of 1. An important feature of BoxMG is bounded complexity in the coarse-grid operator. By exploiting the structure of the problem, BoxMG produces coarse-grid problems with a fixed structure. This results in known communication patterns and guaranteed data locality.

Examining the distributed memory parallel implementation of BoxMG in the

context of parallel scalability, many of the operations are stencil based computations with halo updates. Since the operations are relatively local, they are not expected to significantly limit parallel scalability. For this paper, the particular focus is in parallel decisions at coarse grids. To balance useful local work with communication costs, agglomeration methods are used to redistribute coarse problems. A straightforward approach is agglomeration to one task. This task is then mapped to either a single processor or to all processors redundantly. This method of agglomeration was used in the initial distributed memory implementation of BoxMG; while effective for low processor counts it suffers at scale since the global coarse problem grows linearly with the number of processors. As seen in Figure 1, this is especially true with rectangular local problems for which the coarsest local problem size is larger, and hence, the linear growth is faster and overall parallel scaling is lower. In addition to agglomerating to one task, the coarse problem can be redistributed by agglomerating to n tasks, where n is less than the number of processors. The problem then becomes choosing a desirable value of n which is dependent on the problem distribution on the processor grid. This agglomeration can be applied recursively to gradually reduce the size of the processor grid as the size of the global coarse-grid problem is reduced.

2.2. Redistribution. To extend parallel coarsening in a structured setting, the algorithm introduced in this paper aims to redistribute the coarse-grid problem to an incrementally smaller subset of processors. Parallel coarsening continues until a parameterized minimum local problem size is reached. At this point, a set of possible redistributions is enumerated. These redistributions are evaluated based on a cost derived through a performance model. An optimal redistribution sequence is then selected. It is important to note that since a redistributed problem on a given level also limits parallel coarsening, the selection algorithm is designed to be applied recursively to obtain the highest efficiency possible for the multigrid cycle. Section 4.1 discusses the redistribution of a grid of processors to coarser processor grids.

To redistribute the coarse-grid problem on a smaller number of processors, the processor grid is agglomerated into processor blocks. This agglomeration is performed by dimension to maintain a distributed tensor-product grid structure. Each processor block is then mapped to one task in the redistributed solver.

To map the coarse tasks to processors, two approaches are considered. The first approach uses one processor from each processor block. This is visualized in Figure 3 where the following steps are taken:

1. **Agglomerate:** processors grouped into blocks to define coarse tasks
2. **Gather:** processors within each block perform gather on coarse problem
3. **Cycle:** cycling continues with redistributed problem
4. **Scatter:** iterative solution scattered after redistributed cycle completes

The second approach employs redundancy by mapping each processor in the processor block to the coarse task. This is visualized in Figure 4 with the following steps

1. **Agglomerate:** processors grouped into blocks to define coarse tasks
2. **Allgather:** processors within each block perform allgather on coarse problem
3. **Cycle:** cycling continues redundantly with redistributed problem

While the second approach avoids an additional communication phase at the end of each cycle and adds an opportunity for resilience through redundant cycling, the first approach avoids the increased network usage involved in simultaneous coarse cycles. Algorithm 2 supplements Algorithm 1 with steps needed for redistribution. The algorithm is annotated with parallel communication required for each step.

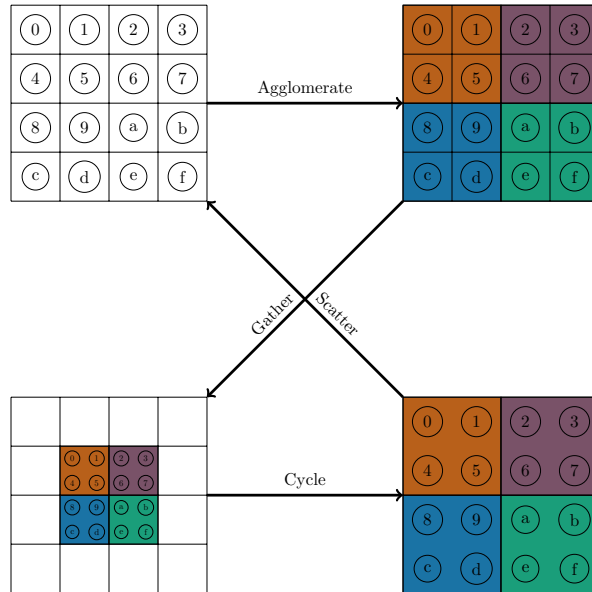


FIG. 3. A redistribution of a 4×4 processor grid to 2×2 processor blocks. The boxes represent the processing elements and the circles represent their respective coarse-grid local problems.

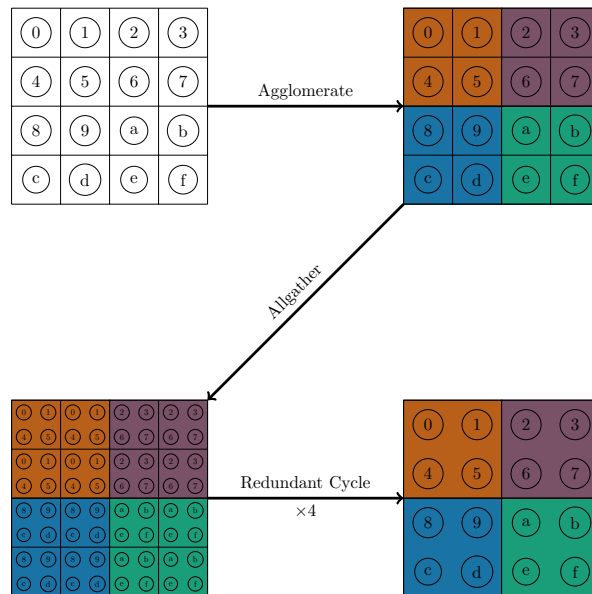


FIG. 4. A redundant redistribution of a 4×4 processor grid to 2×2 processor blocks. The boxes represent the processing elements and the circles represent their respective coarse-grid local problems.

3. Performance Model. In this section, a performance model is introduced for the BoxMG V-cycle (see Algorithm 2). The model helps identify the parallel performance limitations of the V-cycle, particularly at coarse-levels in the multigrid hierarchy, and also provides a cost metric that is used to guide the coarse-level redis-

Algorithm 2: Multilevel V-cycle with Redistribution

Input:	x_{L-1}	fine-grid initial guess
	b_{L-1}	fine-grid right-hand side
	A_0, \dots, A_{L-1}	
	P_1, \dots, P_{L-1}	
	p_0, \dots, p_{L-1}	number of processors on each level
Output: x_{L-1} fine-grid iterative solution		
1	for $l = L - 1, \dots, 1$ do	
2	relax (A_l, x_l, b_l, ν_1)	{halo exchange}
3	$r_l = b_l - A_l x_l$	{halo exchange}
4	$b_{l-1} = P_l^T r_l$	
5	if $p_l > p_{l-1}$	
6	gather_rhs (b_{l-1}, p_l, p_{l-1})	{local gather}
7	$x_0 = \text{solve}(A_0, b_0)$	
8	for $l = 1, \dots, L - 1$ do	
9	if $p_l > p_{l-1}$	
10	scatter_sol (x_{l-1}, p_l, p_{l-1})	{local scatter}
11	$x_l = x_l + P_l x_{l-1}$	{halo exchange}
12	relax (A_l, x_l, b_l, ν_2)	{halo exchange}

tribution algorithm introduced in Section 4.

A key kernel in the V-cycle is that of matrix-vector multiplication. Since the stencil-based computations for this operation are relatively uniform, the cost of parallel communication in matrix-vector multiplication is accurately modeled with a *postal* model [4], leading to a total cost of

$$(1) \quad T = \underbrace{n_f \cdot \gamma}_{\text{computation}} + \underbrace{\alpha + m \cdot \beta}_{\text{communication}},$$

with n_f denoting the number of floating point operations, γ a measure of the computation rate or inverse *effective* FLOP rate, α the interprocessor latency, $1/\beta$ the network bandwidth, and m the number of bytes in an MPI message. The value γ is determined by measuring the computation time of a local stencil-based matrix-vector product, while α and β are determined through standard machine benchmarks such as `mpptest`¹. As an example, the parameters derived for a 9-point 2D stencil on Blue Waters, a Cray XE6 machine at the National Center for Supercomputing Applications², are listed in Table 1. A more accurate model for communication may be used, particularly for multiple communicating cores with large message sizes [15] or to account for network contention [6], which may play a prominent role in communication.

In an L -level multigrid V-cycle, Algorithm 1 is modeled through

$$(2) \quad T_{\text{V-cycle}} = T_{\text{cgsolve}} + \sum_{l=1}^{L-1} T_{\text{smooth}}^l + T_{\text{residual}}^l + T_{\text{restrict}}^l + T_{\text{interp}}^l + T_{\text{agglomerate}}^l.$$

¹<http://www.mcs.anl.gov/research/projects/mpi/mpptest/>

²<https://bluewaters.ncsa.illinois.edu/blue-waters>

α	β	γ
0.65 μ s	5.65 ns/B	0.44 ns/flop

TABLE 1
Model parameters on Blue Waters.

In the following expressions, each component of (2) represents the *actual* implementation and does not necessarily form a minimum bound on each portion of the computation. In the model parameters below, D denotes the number of dimensions in the problem, n_d^l the number of local grid points in dimension d on level l , and n_s the number of points in the stencil. Grid quantities involved in communication and computation are assumed to be 8 byte double-precision floating-point numbers. The dimension of the parallel decomposition is also assumed to match the dimension of the problem. The communication required for a halo exchange of width 1 in D dimensions on level l is modeled as

$$(3) \quad T_{\text{exchange}}^l(D) = 2 \cdot D \cdot \alpha + 2 \cdot \sum_{d=0}^{D-1} n_d^l \cdot 8 \cdot \beta.$$

Smoothing, using Gauss-Seidel with n_c colors, results in

$$(4) \quad T_{\text{smooth}}^l = 2 \cdot n_s \cdot \prod_{d=0}^{D-1} n_d^l \cdot (\nu_1 + \nu_2) \cdot \gamma + n_c \cdot (\nu_1 + \nu_2) \cdot T_{\text{exchange}}^l(D).$$

Likewise, the residual computation is

$$(5) \quad T_{\text{residual}}^l = 2 \cdot n_s \cdot \prod_{d=0}^{D-1} n_d^l \cdot \gamma + T_{\text{exchange}}^l(D).$$

Since it is unnecessary to communicate halo regions in restriction, the computation is entirely local, leading to

$$(6) \quad T_{\text{restrict}}^l = 2 \cdot n_s \cdot \prod_{d=0}^{D-1} n_d^l \cdot \gamma.$$

Following [12], the interpolation and correction computes

$$(7) \quad u^l \leftarrow u^l + I_{l-1}^l u^{l-1} + r^l / C,$$

where r^l is the previously computed residual and C is the center, diagonal stencil coefficient of the operator. Interpolation for edges (see Figure 5) yields

$$(8) \quad u^l \leftarrow \underbrace{u^l + \omega_w u_w^{l-1} + \omega_e u_e^{l-1}}_{5FLOPs} + r^l / C$$

for the x -direction (and similar for the y -direction). Likewise, the interior stencil (see Figure 5) yields

$$(9) \quad u^l \leftarrow \underbrace{u^l + \omega_{sw} u_{sw}^{l-1} + \omega_{se} u_{se}^{l-1} + \omega_{nw} u_{nw}^{l-1} + \omega_{ne} u_{ne}^{l-1}}_{9FLOPs} + r^l / C$$

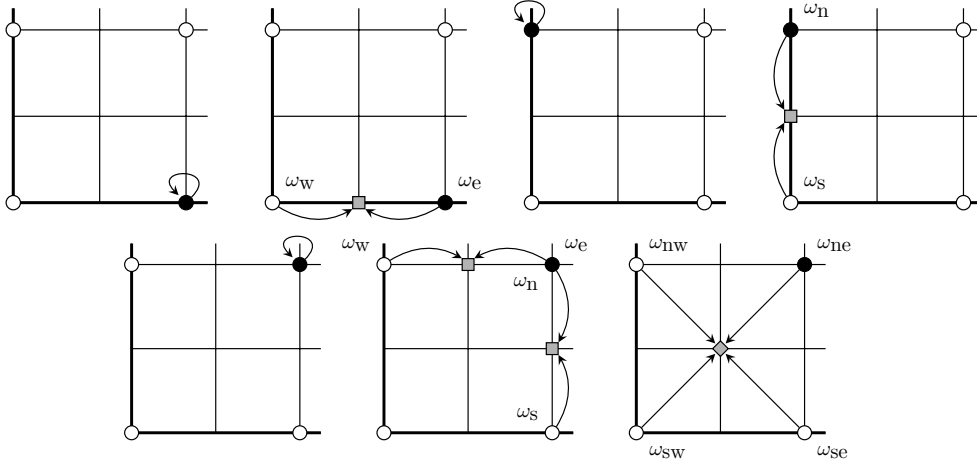


FIG. 5. Interpolation computation in 2D. The top two grids show computation performed on the first coarse line in each dimension. With the exception of the first, each coarse point performs injection to the corresponding fine point. Interpolation to the preceding fine point embedded in the coarse-line is then computed using the surrounding coarse points. The bottom three grids show computation performed for interior coarse points. For each coarse point, the corresponding fine point is injected. The preceding coarse points in each dimension are then interpolated. Finally, the logical cell center preceding the coarse point is interpolated using the surrounding coarse points.

Here interpolation is given as weights stored at the coarse points. For example, the interpolation stencil stored at a given coarse point is

$$\begin{bmatrix} \omega_{nw} & \omega_n & \omega_{ne} \\ \omega_w & & \omega_e \\ \omega_{sw} & \omega_s & \omega_{se} \end{bmatrix}.$$

In total (with injection), interpolation in 2D is modeled as

$$(10) \quad T_{\text{interp}}^l = \left(\prod_{d=0}^1 n_d^l + 20 \cdot \prod_{d=0}^1 n_d^{l-1} + 6 \cdot \sum_{d=0}^1 n_d^{l-1} \right) \cdot \gamma + T_{\text{exchange}}^l(2).$$

Using a similar derivation, interpolation in 3D is

$$(11) \quad T_{\text{interp}}^l = \left(\prod_{d=0}^2 n_d^l + 60 \cdot \prod_{d=0}^2 n_d^{l-1} + 15 \cdot n_0^{l-1} \cdot n_2^{l-1} + 6 \cdot n_1^{l-1} \cdot n_2^{l-1} + n_2^{l-1} \right) \cdot \gamma + T_{\text{exchange}}^l(3).$$

To agglomerate the coarse problem, the right hand side is gathered within processor blocks before the redistributed cycle begins and approximate solution scattered after the redistributed cycle completes. This time is then given by:

$$(12) \quad T_{\text{agglomerate}}^l = \begin{cases} T_{\text{gather_rhs}}^l + T_{\text{scatter_sol}}^l & \text{if } p^l > p^{l-1} \\ 0 & \text{else,} \end{cases}$$

where $T_{\text{gather_rhs}}^l$ and $T_{\text{scatter_sol}}^l$ represent the time to gather and scatter the right-hand side and solution, as follows. The number of processors within a processor block

and the local problem size for a processor in a processor block is given as

$$p_{\text{block}}^l = \prod_{d=0}^{D-1} \left\lceil \frac{p_d^{l+1}}{p_d^l} \right\rceil, \quad n_{\text{block}}^l = \prod_{d=0}^{D-1} \left\lceil \frac{N_d^l}{p_d^l} \right\rceil.$$

Then the solution an MPI `allgather` or `gather/scatter` depends on whether the redistribution is redundant. Following [26], the cost of these collective operations is given by

$$(13) \quad T_{\text{gather_rhs}}^l = \lceil \log_2(p_{\text{block}}^l) \rceil \cdot \alpha + n_{\text{block}}^l \cdot \frac{p_{\text{block}}^l - 1}{p_{\text{block}}^l} \cdot 8\beta$$

$$(14) \quad T_{\text{scatter_sol}}^l = \begin{cases} 0 & \text{if redundant} \\ T_{\text{gather_rhs}}^l & \text{else.} \end{cases}$$

Finally, the time for a coarse solve is the time to agglomerate to one processor combined with the cost of a Cholesky direct solve:

$$(15) \quad T_{\text{cgsolve}} = T_{\text{agglomerate}}^0 + \left(\prod_{d=0}^{D-1} N_d^0 \right)^2 \cdot \gamma.$$

This assumes the Cholesky factorization has been computed and stored in the setup phase.

This performance model provides a basic predictive model to begin exploring the guided redistribution algorithm proposed in this paper.

4. Optimized Parallel Redistribution Algorithm.

4.1. Coarse Processor Grid Enumeration. To enumerate potential redistributions, the fine-grid tasks described by the processor grid are agglomerated into coarser tasks called processor blocks. In agglomerating by dimension, the processor blocks form a coarser tensor product grid. The coarse processor grids are enumerated by beginning with a 1-D grid and by refining greedily by dimension with respect to the agglomerated local problem size. Using a refinement factor of 2, the number of enumerated processor grids is bounded by $\lceil \log_2 n_p \rceil$. Table 2 illustrates this enumer-

Redistribution	Agglomerated Local Problem
1×1	1136×71
2×1	568×71
4×1	284×71
8×1	142×71
16×1	71×71
16×2	71×36
16×4	71×18

TABLE 2

Example redistribution enumeration using a fine grid problem of 9088×568 degrees of freedom with a 16×8 processor grid. The global coarse-grid considered for agglomeration contains 1136×71 degrees of freedom.

ation strategy using an initial fine grid problem of 9088×568 degrees of freedom with a 16×8 processor grid. This refinement procedure is used to limit the number of potential redistributions thereby making the global search feasible within the setup phase.

4.2. Redistribution Search. The recursive enumeration of coarse processor grids generates a search space of possible redistributions. To find an optimal redistribution, a state in the search space is given by the size of the processor grid and the size of the coarse-grid associated with a distributed solver. The search space can be viewed as a directed graph — an example is given in Figure 6. The initial state is given by the top-level distributed solver and the goal state is the state with a 1×1 processor grid (in the case of a 2-D problem). State transitions have varying costs; the goal is an inexpensive path from the initial state to the goal state.

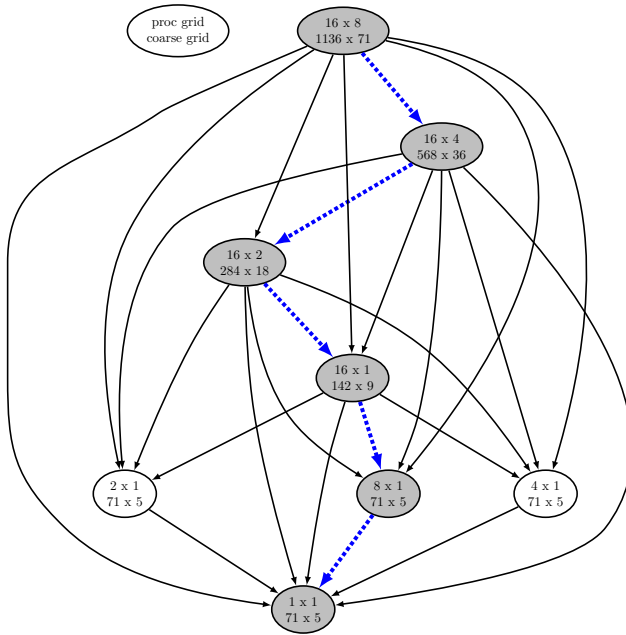


FIG. 6. *Example redistribution search space: The fine grid global problem is 9088×568 degrees of freedom with a 16×8 processor grid, yielding a fine grid local problem of 568×71 . The optimal path through this redistribution space is highlighted.*

To search the state space, a path cost function is defined as

$$(16) \quad f(s) = g(s) + h(s)$$

where s is a vertex or state in the graph in Figure 6, g is the cost to reach s from the initial state, and h is an estimate of the cost to reach the goal state from state s . That is, $g(s)$ represents the time predicted by the performance model for a solve phase executed down to coarse-grid state s . For the heuristic function $h(s)$, a weighted combination of the coarse-grid problem and the processor grid size is used to predict the cost. If the performance model is an accurate predictive model, an inexpensive path from the initial state to the goal state will identify a redistributed solver with an efficient run-time. With the path cost function defined, the space of redistributions is searched for an optimal path. This is performed in the MG setup phase to dictate

agglomeration when a coarsening limit is reached. Using a brute force approach by searching every path for the best redistribution strategy incurs an $\mathcal{O}(n_p)$ cost, since the redistribution search space is constructed recursively. Letting $h = \log_2(n_p)$, and using the above coarse processor grid enumeration, results in

$$(17) \quad T(0) = 1, \quad T(h) = \sum_{k=0}^{h-1} T(k) + 1.$$

Since $2^0 = T(0) = 1$ and since

$$\begin{aligned} T(h+1) &= \sum_{k=0}^h T(k) + 1 \\ &= T(h) + \sum_{k=0}^{h-1} T(k) + 1 \\ &= 2^h + 2^h = 2^{h+1}, \end{aligned}$$

this leads to $T(h) = 2^h = 2^{\log_2(n_p)} = n_p$.

To address the $\mathcal{O}(n_p)$ cost, the A* algorithm is used to determine the optimal path. While the worst case complexity for A* is $\mathcal{O}(n_p)$ for this search, the cost with an optimal heuristic with evaluation cost $\mathcal{O}(1)$ is the length of the solution path. The length of this path in the redistribution search is $\mathcal{O}(\log_2(n_p))$. Figure 7 shows the A* heuristic is effective in avoiding the brute force complexity, but does not reach the optimal complexity.

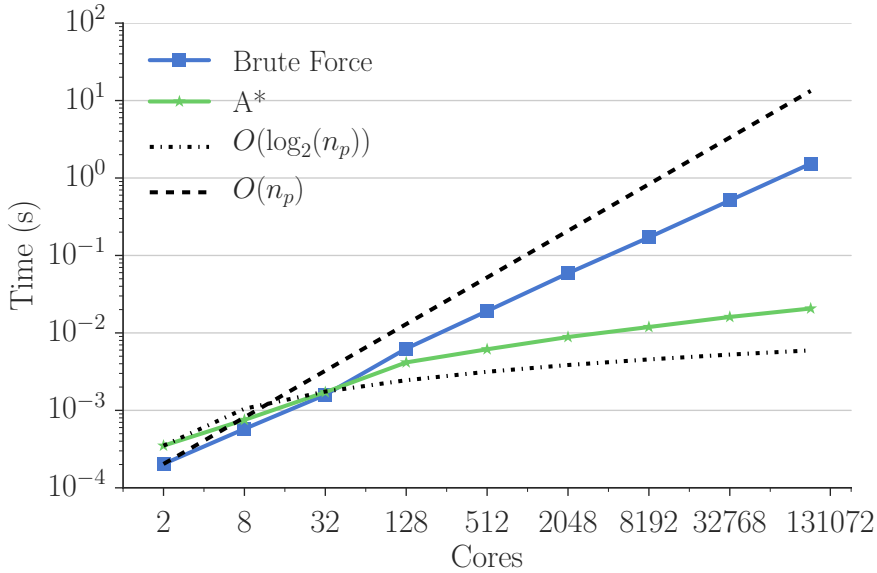


FIG. 7. Performance of redistribution search algorithms weak scaling with local problem size 568×71 .

5. Experimental results. To explore the performance of the proposed redistribution algorithm a standard 5-point finite volume discretization of the diffusion

equation is used. Since square problems may lead to a natural or predictable redistribution path, rectangular local problems are used in order to fully stress the redistribution algorithm in a weak scaling study. In particular, the ratio of processors in the processor grid is fixed at 2 : 1, and the ratio of unknowns in the fine-grid local problem is fixed at 8 : 1. Other processor grid ratios lead to similar findings.

Note that for an isotropic diffusion problem this grid stretching results in anisotropy in the discrete problem, causing the convergence of the solver to deteriorate when using point-wise smoothing. Consequently, a diffusion problem with compensating *anisotropy* is defined in order to focus on the parallel scalability of the coarse-grid redistribution algorithm (rather than the well-established convergence rate of the multigrid algorithm itself). Specifically, the following diffusion problem is used in these numerical experiments,

$$(18) \quad -\nabla \cdot (D\nabla u) = f(x, y) \quad \text{in } \Omega = (0, 1) \times (0, 1),$$

$$(19) \quad u = 0 \quad \text{on } \partial\Omega,$$

where the diffusion tensor is $D = \text{diag}[\frac{1}{r}, r]$ and $r \approx 16$. This compensating anisotropy results in optimal convergence of multigrid V-cycles with point-wise smoothing.

5.1. Scaling Studies. Both the weak and strong scalability of multigrid V-cycles that use the proposed redistribution algorithm are important for applications on exascale systems. Here, the discretization of the diffusion problem given above is used for both weak and strong scaling studies and the algorithmic components of the BoxMG multigrid library (e.g., interpolation, restriction) are used in the redistributed multigrid V-cycles.

Since, the cost of coarsening (with redistribution) and the cost of the coarse-grid problem are dominated by parallel communication, network speed and machine topology play an important role in timings. To explore this dependency, two different petascale systems are considered in the scaling tests:

Mira³ An IBM Blue Gene/Q system at Argonne National Laboratory. Mira uses an IBM network which comprises a 5D torus with 49,152 compute nodes using PowerPC A2 processors.

Blue Waters⁴ A Cray XE system at the National Center for Supercomputing Applications (NCSA) at the University of Illinois at Urbana-Champaign. Blue Waters employs a 3D torus using a Cray Gemini interconnect and has 22,640 XE compute nodes each with two AMD Interlagos processors.

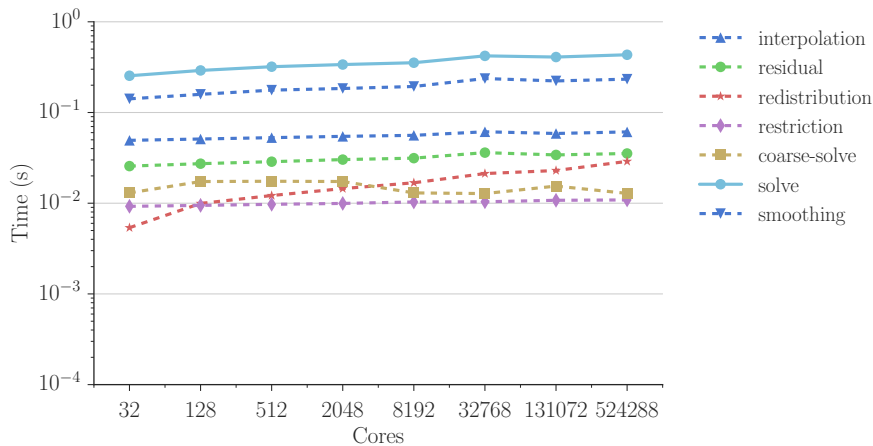
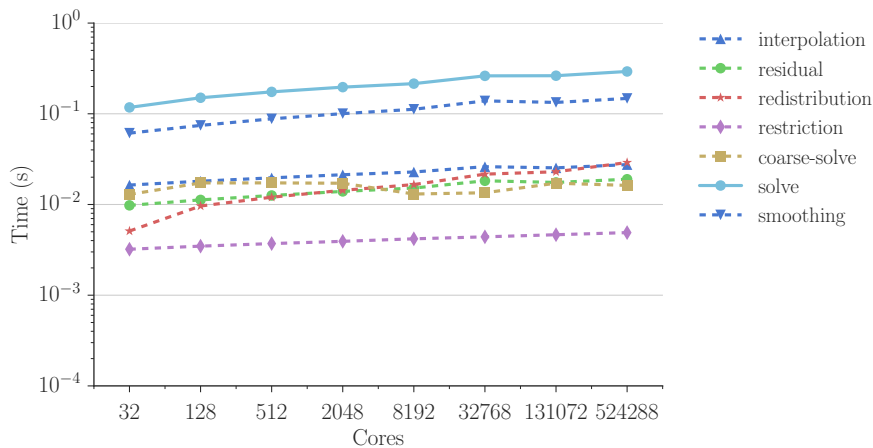
In each case, the machine parameters used in the performance model of Section 3 are determined using the b_{eff} benchmark [24].

Weak Scalability. In this section, a weak scaling study is conducted to highlight the scalability of the redistribution algorithm at large core counts. For the numerical experiments below, 10 V(2,1)-cycles are executed using two different local problems sizes: $568 \times 71 = 40,328$ and $288 \times 36 = 10,368$.

Figures 8 and 9 show the run times on Mira of various computational kernels in the multigrid solve phase. The redistribution line shows communication needed to redistribute coarse problems. This communication is low in comparison to the cost of relaxation. Overall, the algorithm exhibits high parallel scalability in the solve time for both local problem sizes on Mira.

³<https://www.alcf.anl.gov/mira>

⁴<https://bluwaters.ncsa.illinois.edu/blue-waters>

FIG. 8. Weak scaling on Mira with local problem size: 568×71 .FIG. 9. Weak scaling on Mira with local problem size: 288×36 .

With different network capacities, *redundant* redistribution may not yield the lowest communication costs. Indeed, the results in Figure 10 for the Blue Waters system show that while redundant redistribution of the data at course levels is inexpensive, the network contention introduced by redundant cycling contributes to an increase in communication at high core counts. This suggests that triggering redundancy on a per-level basis could lead to reduced costs. In contrast, non-redundant redistribution (in Figure 10) exhibits high scalability — thus, it is used for the following runs on Blue Waters.

Figures 11 and 12 show run times on Blue Waters for the multigrid solve phase, highlighting that the proposed algorithm achieves good parallel scalability here as well. However, comparing runs on the two machines, it is apparent that the weak scalability is superior on Mira. This is attributed to the network capabilities and scheduling differences of the two machines. Jobs on Mira receive a dedicated, full torus partition of the machine, which often reduces contention resulting from neighboring jobs on the machine, since partitions receive a full torus network. Moreover, the lower

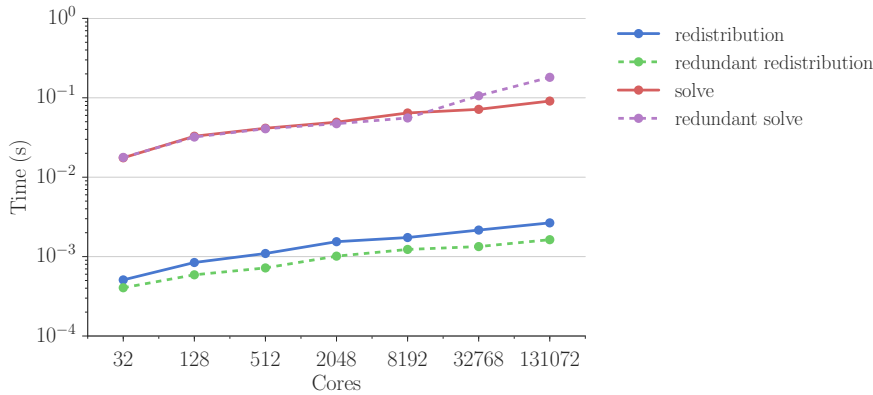


FIG. 10. Weak scaling on Blue Waters with local problem size 288×36 shows the significant improvement of non-redundant redistribution compared to redundant redistribution beyond 8192 cores.

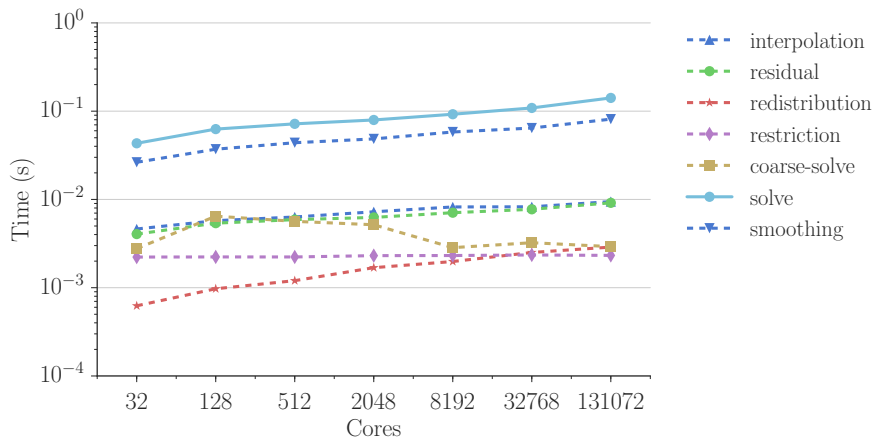


FIG. 11. Weak scaling on Blue Waters with local problem size: 568×71 .

dimensional 3D torus on Blue Waters also contributes to an increase in contention within the running job.

Nevertheless, on Blue Waters communication cost for redistribution remains relatively low in comparison to smoothing, which remains the dominant kernel in the overall solve. Figure 13 decomposes the cost of smoothing into communication and computation. This decomposition indicates that the communication cost of the halo exchange is the primary contributor to the reduced scalability.

In contrast to the network advantages of Mira, lower floating point performance is observed for the key computational kernels on Mira than on Blue Waters. This difference, combined with an extra core dedicated to operating system functions, yields more predictable performance and superior scaling behavior. This is also observed for a variety of applications [18]: loss in performance on the Cray XE6 in comparison to BG/Q systems as the core count increases. However, with the data locality and fixed communication patterns of the algorithm, the network performance on Blue Waters is good enough to let its superior floating performance yield the best time to solution, solving approximately 2.5 times faster at 131K cores.

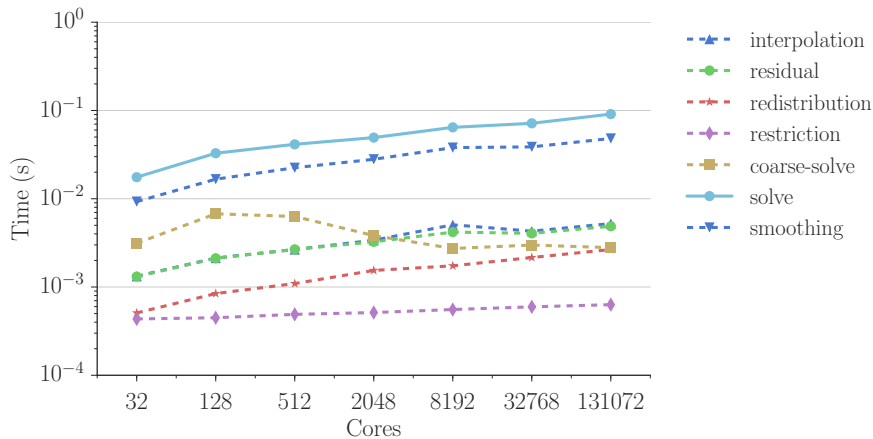


FIG. 12. Weak scaling on Blue Waters with local problem size: 288×36 .

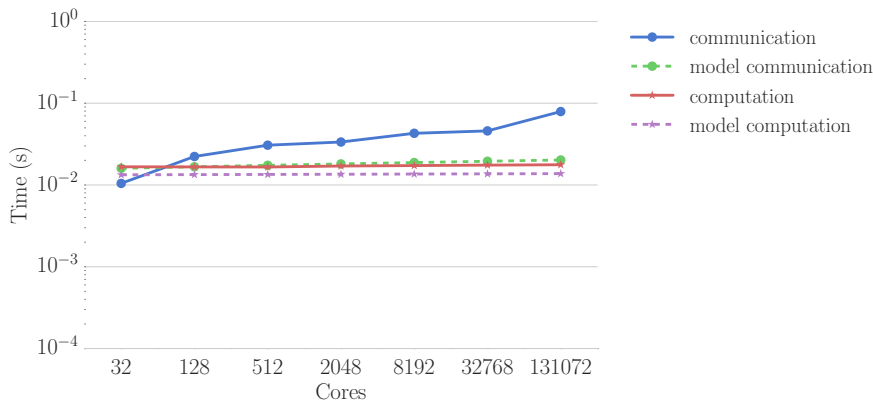


FIG. 13. Weak scaling of smoothing routine on Blue Waters with local problem size 568×71 .

Strong Scalability. Turning to strong scalability, an isotropic model diffusion problem is setup on a 3200×3200 grid, and then executed on a sequence of square processor grids. The number of cores in each coordinate direction is successively doubled from 8 to 128, to create a range of core counts from 64 to 16,384, with a corresponding local problem size ranging from 160,000 to 625 degrees of freedom (dof). The strong scaling performance for Blue Waters is shown in Figure 14. Here, the strong scaling limit is reached at 1024 cores, which is equivalently 10K dof per core. This scaling limit is consistent with other performance assessments of multilevel solvers in application codes (e.g., [16, 25]).

The computational cost of the solve is again dominated by smoothing and scaling is limited by communication, as supported in Figure 13 by the performance model of Section 3. Often a hybrid Gauss-Seidel Jacobi sweep is used to limit communication to once per relaxation sweep [3], improving the cycles strong scaling even though it may potentially slow convergence. Here, the focus is on redistribution and the impact of communication is highlighted with a strict implementation of four-color Gauss-Seidel, which results in four halo exchanges per relaxation sweep. The granularity of the component timers is such that the residual and interpolation operations each include

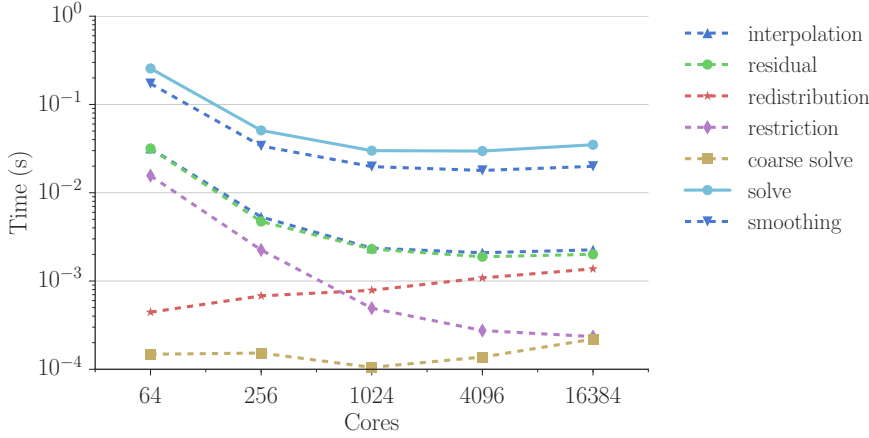


FIG. 14. Strong scaling on Blue Waters with problem size: 3200×3200 .

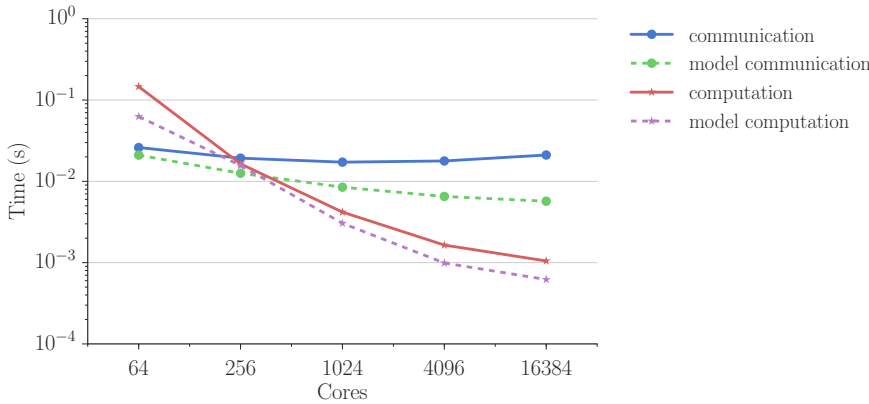


FIG. 15. Strong scaling of smoothing routine on Blue Waters with problem size: 3200×3200 .

a single halo exchange. This leads to strong scaling curves for these operations that are very similar to smoothing, but much faster in absolute terms.

In contrast, the restriction has no communication, and would exhibit perfect strong scaling in the absence of redistribution. With redistribution fewer cores are used at coarser levels, and strong scaling begins to degrade at 2.5K dof per core, although speedup is still realized even at 625 dof per core. This observation highlights the complexity of trade-offs in multilevel algorithms on modern systems, and the important role of performance models in design and runtime optimization.

5.2. Performance of Optimized Redistribution. To understand the impact of the redistribution path on solve time, the 568×71 weak scaling problem used in Figure 11 with 2048 processors is executed over a variety of redistribution choices. The selected redistribution paths are listed in Table 3. Path 1 indicates the optimal redistribution path used in Figure 11 and is selected by the algorithm from Section 4. In stark contrast to Path 1 is Path 0, which is the original all-to-one redistribution path that is known to scale poorly. The remaining paths highlight the flexibility in the agglomeration sequence.

Path	Processor Grid Redistribution
0	$64 \times 32 \rightarrow 1 \times 1$
1	$64 \times 32 \rightarrow 64 \times 16 \rightarrow 64 \times 8 \rightarrow 64 \times 4 \rightarrow 32 \times 2 \rightarrow 16 \times 1 \rightarrow 1 \times 1$
2	$64 \times 32 \rightarrow 64 \times 4 \rightarrow 8 \times 1 \rightarrow 4 \times 1$
3	$64 \times 32 \rightarrow 16 \times 2 \rightarrow 1 \times 1$
4	$64 \times 32 \rightarrow 64 \times 16 \rightarrow 2 \times 1 \rightarrow 1 \times 1$
5	$64 \times 32 \rightarrow 4 \times 1 \rightarrow 1 \times 1$
6	$64 \times 32 \rightarrow 64 \times 16 \rightarrow 4 \times 1 \rightarrow 1 \times 1$
7	$64 \times 32 \rightarrow 64 \times 16 \rightarrow 64 \times 8 \rightarrow 2 \times 1 \rightarrow 1 \times 1$
8	$64 \times 32 \rightarrow 2 \times 1 \rightarrow 1 \times 1$

TABLE 3

Example redistribution paths using a 64×32 processor grid and 568×71 local problem size.

The bar graph in Figure 16 compares the run times and predicted times of the multigrid solve phase for the various redistribution paths shown in Table 3. The predicted times are computed using the performance model from Section 3, and are in good agreement with the actual run times. Comparing the run times of Path 0 and Path 1, this graph shows a 40 times speedup of the new redistribution strategy over the original all-to-one strategy. In addition, Path 1 has the lowest run time of several plausible alternatives to the all-to-one strategy. Thus, Figure 16 demonstrates the utility of using a global search guided by a performance model as a predictive tool for choosing optimal redistribution paths. Moreover, using this strategy to select the redistribution path delivered effective weak parallel scaling out to 500K+ cores on Mira, and out to 132K+ cores on Blue Waters, while the original code was essentially unusable beyond 4K cores.

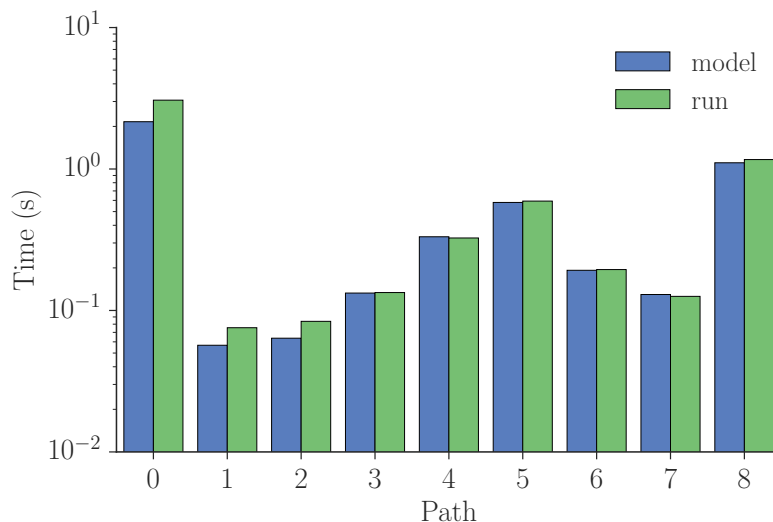


FIG. 16. *Model and run times on Blue Waters of various redistribution paths using a 64×32 processor grid and 568×71 local problem size.*

6. Conclusions. Emerging architectures place an increasing importance on data locality and minimizing data movement. In these environments, structured approaches benefit from predictable memory access patterns and avoiding indirect addressing. This motivates the development of methods that exploit local structure to avoid incurring the performance consequences of full algebraic generality. A robust structured single-block multigrid implementation that scales well on modern architectures is an important step toward this goal.

In this paper, a new optimized recursive agglomeration algorithm for redistributing coarse-grid work in structured multilevel solvers is introduced. This algorithm combines a predictive performance model with a structure exploiting recursive enumeration of coarse processor grids to enable a global search for the optimal agglomeration strategy. This approach significantly improves the weak parallel scalability of robust, structured multigrid solvers such as BoxMG. In this study using BoxMG operators, this new algorithm delivers very good weak scaling up to 524,288 cores on an IBM BG/Q (Mira), and reasonable weak scaling up to 131,072 cores on Cray XE (Blue Waters). The speedup over the previous all-to-one agglomeration approach is significant even at modest core counts, 40 times speedup on just 2048 cores and 144 times speedup on 8192 cores. At larger core counts, the all-to-one agglomeration approach became infeasible as the increased memory requirements for the coarse-grid problem exceeded available memory.

In addition, the strong scaling of multigrid solves using this redistribution algorithm is demonstrated on Blue Waters. Overall, the scaling limit is observed to be approximately 10K dofs per core, which is similar to results obtained in other studies and is dominated by the communication cost of the smoother. Future work on additive variants of multigrid and improvements to the performance model to more accurately capture deep memory hierarchies are needed to reduce this limit.

To focus on coarse-grid redistribution, only pointwise Gauss-Seidel relaxation is considered in this paper. In the future, smoothers that may enhance performance, such as hybrid or polynomial smoothers, or enhance robustness, such as line and plane smoothers [2], may be considered and their impact on optimal coarse-grid redistribution explored.

Acknowledgments. This work was carried out under the auspices of the National Nuclear Security Administration of the U.S. Department of Energy, at the University of Illinois at Urbana-Champaign under Award Number DE-NA0002374, and at Los Alamos National Laboratory under Contract Number DE-AC52-06NA25396, and was partially supported by the Advanced Simulation and Computing / Advanced Technology Development and Mitigation Program. This research is part of the Blue Waters sustained-petascale computing project, which is supported by the National Science Foundation (awards OCI-0725070 and ACI-1238993) and the state of Illinois. Blue Waters is a joint effort of the University of Illinois at Urbana-Champaign and its National Center for Supercomputing Applications. This research used resources of the Argonne Leadership Computing Facility, which is a DOE Office of Science User Facility supported under Contract DE-AC05-00OR22725.

REFERENCES

- [1] R. E. ALCOUFFE, A. BRANDT, J. E. DENDY, AND J. W. PAINTER, *The multi-grid method for the diffusion equation with strongly discontinuous coefficients*, SIAM J. Sci. Stat. Comput., 2 (1981), pp. 430–454.
- [2] T. M. AUSTIN, M. BERNDT, AND J. D. MOULTON, *A memory efficient parallel tridiagonal*

- solver*, Tech. Report LA-UR 03-4149, Mathematical Modeling and Analysis Group, Los Alamos National Laboratory, Los Alamos, NM, 2004.
- [3] A. H. BAKER, R. D. FALGOUT, H. GAHVARI, T. GAMBLIN, W. GROPP, T. V. KOLEV, K. E. JORDAN, M. SCHULZ, AND U. M. YANG, *Preparing algebraic multigrid for exascale*, Tech. Report LLNL-TR-533076, Lawrence Livermore National Laboratory, Lawrence Livermore, CA, 2012.
 - [4] A. BAR-NOY AND S. KIPNIS, *Designing broadcasting algorithms in the postal model for message-passing systems*, in Proceedings of the Fourth Annual ACM Symposium on Parallel Algorithms and Architectures, SPAA '92, New York, NY, USA, 1992, ACM, pp. 13–22, <https://doi.org/10.1145/140901.140903>, <http://doi.acm.org/10.1145/140901.140903>.
 - [5] A. BIENZ, R. D. FALGOUT, W. GROPP, L. N. OLSON, AND J. B. SCHRODER, *Reducing parallel communication in algebraic multigrid through sparsification*, SIAM J. Sci. Comput., 38 (2016), pp. S332–S357, <https://doi.org/10.1137/15M1026341>, <https://doi.org/10.1137/15M1026341>.
 - [6] A. BIENZ, W. D. GROPP, AND L. OLSON, *Topology-aware performance modeling of parallel spmv*s. http://meetings.siam.org/sess/dsp_talk.cfm?p=75934.
 - [7] A. BRANDT, S. F. MCCORMICK, AND J. W. RUGE, *Algebraic multigrid (amg) for sparse matrix equations*, Sparsity and Its Applications, (1984).
 - [8] W. L. BRIGGS, V. E. HENSON, AND S. F. MCCORMICK, *A Multigrid Tutorial: Second Edition*, Society for Industrial and Applied Mathematics, Philadelphia, PA, USA, 2000.
 - [9] G. L. DELZANNO, L. CHACÓN, J. M. FINN, Y. CHUNG, AND G. LAPENTA, *An optimal robust equidistribution method for two-dimensional grid adaptation based on mongekantorovich optimization*, Journal of Computational Physics, 227 (2008), pp. 9841–9864, <https://doi.org/http://dx.doi.org/10.1016/j.jcp.2008.07.020>, <http://www.sciencedirect.com/science/article/pii/S0021999108004105>.
 - [10] J. E. DENDY, *Black box multigrid*, J. Comput. Phys., 48 (1982), pp. 366–386.
 - [11] J. E. DENDY, *Black box multigrid for nonsymmetric problems*, Appl. Math. Comput., 13 (1983), pp. 261–283.
 - [12] J. E. DENDY AND J. D. MOULTON, *Black box multigrid with coarsening by a factor of three*, J. Numer. Lin. Alg. App., 17 (2010), pp. 577–598, <https://doi.org/10.1002/nla.705>.
 - [13] H. GAHVARI, W. GROPP, K. E. JORDAN, M. SCHULZ, AND U. M. YANG, *Systematic reduction of data movement in algebraic multigrid solvers*, in Proceedings of the 2013 IEEE 27th International Symposium on Parallel and Distributed Processing Workshops and PhD Forum, IPDPSW '13, Washington, DC, USA, 2013, IEEE Computer Society, pp. 1675–1682.
 - [14] W. GROPP, *Parallel computing and domain decomposition*, in Domain Decomposition Methods for Partial Differential Equations, Norfolk, VA, USA, 1992, Society for Industrial & Applied Mathematics, pp. 349 – 361.
 - [15] W. GROPP, L. N. OLSON, AND P. SAMFASS, *Modeling MPI communication performance on SMP nodes: Is it time to retire the ping pong test*, in Proceedings of the 23rd European MPI Users' Group Meeting, EuroMPI 2016, New York, NY, USA, 2016, ACM, pp. 41–50, <https://doi.org/10.1145/2966884.2966919>, <http://doi.acm.org/10.1145/2966884.2966919>.
 - [16] G. E. HAMMOND, P. C. LICHTNER, C. LU, AND M. R.T., *Pflotran: Reactive flow and transport code for use on laptops to leadership-class supercomputers*, in Groundwater Reactive Transport Models, F. Zhang, G. Yeh, and J. C. Parker, eds., Bentham Science Publishers, Sharjah, UAE, 2012, pp. 141–159, <https://doi.org/10.2174/97816080530631120101>.
 - [17] W. JOUBERT AND J. CULLUM, *Scalable algebraic multigrid on 3500 processors*, Electron. T. Numer. Ana., 23 (2006), pp. 105–128.
 - [18] D. J. KERBYSON, K. J. BARKER, A. VISHNU, AND A. HOISIE, *Comparing the performance of Blue Gene/Q with leading Cray XE6 and InfiniBand systems*, Proceedings of the International Conference on Parallel and Distributed Systems - ICPADS, (2012), pp. 556–563, <https://doi.org/10.1109/ICPADS.2012.81>.
 - [19] S. P. MACLACHLAN AND J. D. MOULTON, *Multilevel upscaling through variational coarsening*, Water Resour. Res., 42 (2006), W02418, <https://doi.org/10.1029/2005WR003940>.
 - [20] S. P. MACLACHLAN, J. M. TANG, AND C. VUIK, *Fast and robust solvers for pressure-correction in bubbly flow problems*, J. Comput. Phys., 227 (2008), pp. 9742–9761.
 - [21] D. MOULTON, L. N. OLSON, AND A. REISNER, *Cedar framework*, 2017, <https://github.com/cedar-framework/cedar>. Version 0.1, release paperwork in process at LANL.
 - [22] J. D. MOULTON, J. E. DENDY, AND J. M. HYMAN, *The black box multigrid numerical homogenization algorithm*, J. Comput. Phys., 141 (1998), pp. 1–29.
 - [23] K. NAKAJIMA, *Optimization of serial and parallel communications for parallel geometric multigrid method*, in 2014 20th IEEE International Conference on Parallel and Distributed Systems (ICPADS), Dec 2014, pp. 25–32.

- [24] R. RABENSEIFNER, *Effective bandwidth (b_{eff}) benchmark*, www.hlrs.de/mpi/b_eff.
- [25] H. SUNDAR, G. BIROS, C. BURSTEDDE, J. RUDI, O. GHATTAS, AND G. STADLER, *Parallel geometric-algebraic multigrid on unstructured forests of octrees*, in Proceedings of the International Conference on High Performance Computing, Networking, Storage and Analysis, IEEE Computer Society Press, 2012, p. 43.
- [26] R. THAKUR, R. RABENSEIFNER, AND W. GROPP, *Optimization of collective communication operations in MPICH*, International Journal of High Performance Computing Applications, 19 (2005), pp. 49–66.
- [27] U. TROTTEMBERG AND A. SCHULLER, *Multigrid*, Academic Press, Inc., Orlando, FL, USA, 2001.
- [28] D. E. WOMBLE AND B. C. YOUNG, *A MODEL AND IMPLEMENTATION OF MULTIGRID FOR MASSIVELY PARALLEL COMPUTERS*, International Journal of High Speed Computing, 2 (1990), pp. 239–255.
- [29] P. D. ZEEUW, *Matrix-dependent prolongations and restrictions in a blackbox multigrid solver*, Journal of Computational and Applied Mathematics, 33 (1990), pp. 1–27, [https://doi.org/10.1016/0377-0427\(90\)90252-U](https://doi.org/10.1016/0377-0427(90)90252-U).